# Impact of gas flow on dielectric barrier discharge for air purification

B. Mahdavipour[1], R. Zaplotnik[2], M. Panjan[3], J. Oberrath[1] and S. Dahle[4,5]

[1]*Modelling within Local Engineering, Institute of Product and Process Innovation, Leuphana University Lüneburg, Germany*
[2]*Department of Surface Engineering and Optoelectronics, Jožef Stefan Institute, Slovenia*
[3]*Department of Thin Films and Surfaces, Jožef Stefan Institute, Slovenia*
[4]*Department of Wood Science and Technology, Biotechnical faculty, University Ljubljana, Ljubljana, Slovenia*
[5]*Clausthal Center of Materials Technology, Clausthal University of Technology, Clausthal-Zellerfeld, Germany*

**Abstract:** We investigated the effect of airflow on a dielectric barrier discharge (DBD) plasma via electrical measurements, optical emission spectroscopy and fast video analysis. Using microsecond pulses yielded significant differences from sinusoidal high voltage excitation. Observations confirmed immanent changes in discharge appearance and homogeneity, but also in reduced electric field strength, peak voltages and transferred power.

**Keywords:** dielectric barrier discharge, air purification

## 1. Introduction

DBDs have been applied to a variety of applications such as ozone generation, wood treatment, plasma medicine, as well as for gas treatment and pollution control. Planar DBDs are the most common devices among the DBD configurations. Due to their geometry, they allow for an easy access to perform optical spectroscopy and low rate calculations. Few studies have been done about the gas flow influence on the filament discharges in DBDs [1]. Total gas flow effects on the electrical parameters of discharge and also sometimes on the filament diameter. However, due to the different time scales of the discharges, it is difficult to argue that the gas flow has a direct effect on the filaments ignition.

The aim of this research is to gain further insight on the effects of gas flow on the behaviour of an air DBD plasma setup, which was developed for exhaust air purification [2].

## 2. Experimental

The discharge system was comprised of a dielectrically insulated electrode provided by PlasmaGreen GmbH, which was positioned in-between two stainless steel sheets. The area of the plasma discharge amounts to 400 cm². A 120 mm fan (Sunon DP201A2123HST) with a custom-fitted air channel provided the stable gas flow through the plasma setup. The velocity of the gas flow was measured using a commercial probe (Trotec TA300). The complete system is depicted in Fig. 1, drawings of the setup with all measurements have been made available [3].

A commercial Fourier-synthesis high voltage pulse power supply (Ingenieurbüro Dr. Jürgen Klein, S/N 040-3) and a pre-commercial high voltage power supply (control unit PG040B-0001 with high voltage unit PG040C-0001, PlasmaGreen GmbH, Germany) were used as pulsed and sinusoidal power supplies, respectively. Figure 2 shows the voltage graph of both power supplies. Further, for the sinusoidal power supply, experiments were done in two different setups: In one setup, the electrode was grounded, and in another one it was floating. In all experiments, power supplies were connected to the dielectrically insulated electrode. All optical measurements were carried out through a transparent sidewall.

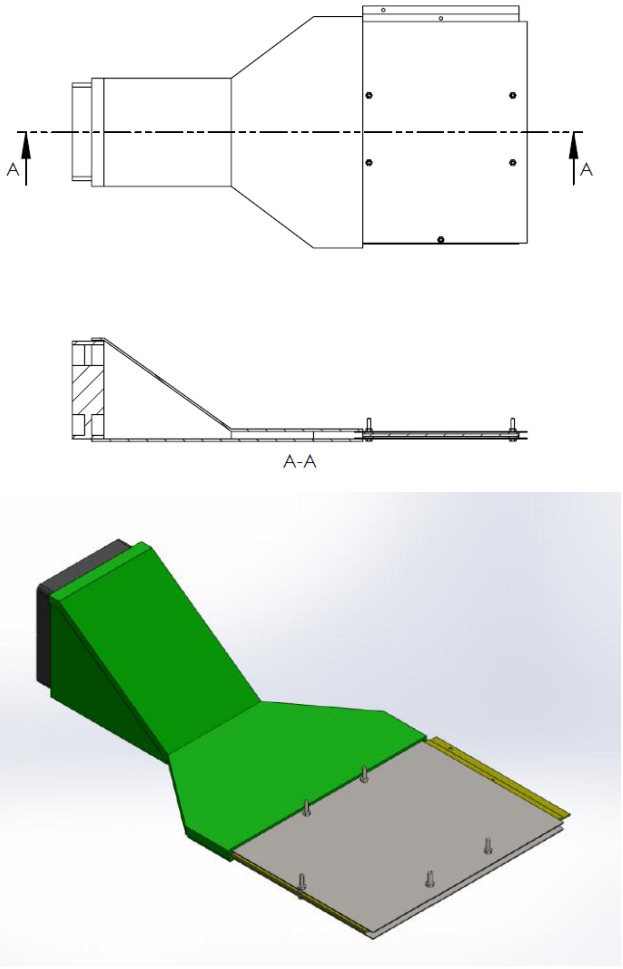


Fig. 1. Schematic drawings of the plasma setup from above (top image), as sectional view from the side (middle image), and as three-dimensional model in isometric view (bottom image).

Fig. 2 depicts the high voltage signals from the pulsed power supply (red line, signal starting at 50 µs) and the sinusoidal power supply (black line, signal starting 100 µs earlier). The pulsed HV peaks have an average width at half maximum of 0.6 µs, followed by approx. 50 µs of oscillations at a pattern typical for Fourier synthesis, while

no potentials are present in-between the individual HV pulses. The sinusoidal power supply exhibits alternating HV peak heights, every second pulse being reduced by approx. 11 %. Further, the potential in-between first and second pulse is staying on an elevated level, depleting slowly from 67 % down to 45 % of the maximum potential. In contrast, the potential drops to its initial, minimum value after each second pulse. This behaviour indicates the presence of many harmonics of the original excitation frequency in the system. Most probably, the specific shape originates in a coupled oscillation of secondary circuit (high voltage side including reactor) and primary circuit (internal driving stage of the power supply).

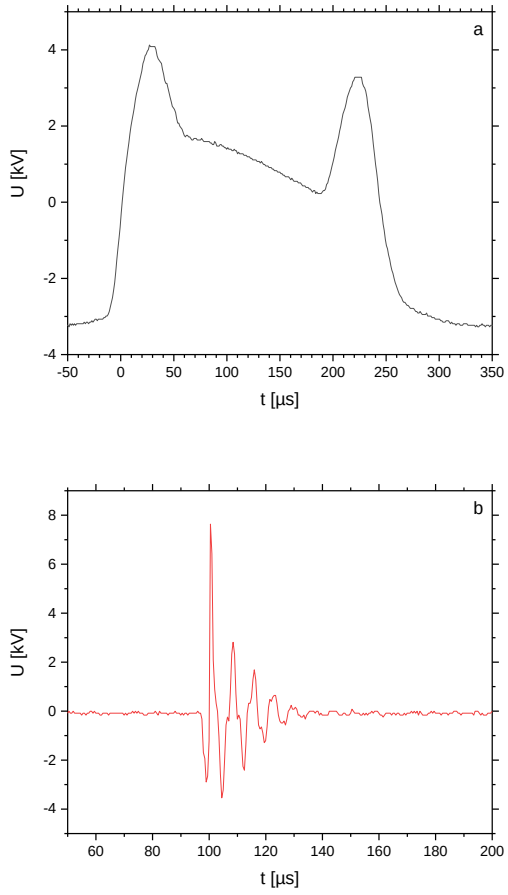


Fig. 2. Example voltage slopes for both, the sinusoidal (a) and the pulsed high voltage power supply (b).

Regarding the applications for gas purification, typical devices are electrically connected in two different ways, either grounding every second electrode in a stack or keeping the whole stack on a floating potential by not including connections to physical earth potential at any electrode. Both type of connections were tested for the sinusoidal power supply.

The resulting plasma discharges were characterized using a commercial 100 MHz, 1000:1, 40 kV passive high voltage probe (Datatec PHV-4002-3-RO) and an inductive DC current probe (Datatec N2893A) together with a digital oscilloscope (Keysight DSOX3024T with upgrade DSOX3MSO). Power calculations were performed by integrating potential differences between the electrodes and time-dependent discharge currents over several milliseconds.

Optical emission spectroscopy (OES) were carried out using a 16-bit Avantes AvaSpec 3648 fibre optic spectrometer (Avantes Inc., Louisville, CO, USA). Reduced electric fields have been evaluated from the nitrogen emission lines $N_2^+$ ($B^2\Sigma_u^+ \rightarrow X^2\Sigma_g^+$, (0, 0)) at 391.4 nm and $N_2$ ($C^3\Pi_u \rightarrow B^3\Pi_g$, (2, 5)) at 394.3 nm after Paris and colleagues [4,5,6,7]. The distribution of filaments was investigated via a high-speed camera (Photron Fastcam SA-Z).

## 3. Results and discussion

The electrical characterization of the plasma discharge using both power supplies and different experimental conditions is shown in Fig. 3. Light orange bars represent peak-to-peak voltages and black bars depict the average electrical power transfer into the discharge for all samples with a proper ground connection to physical earth potential.

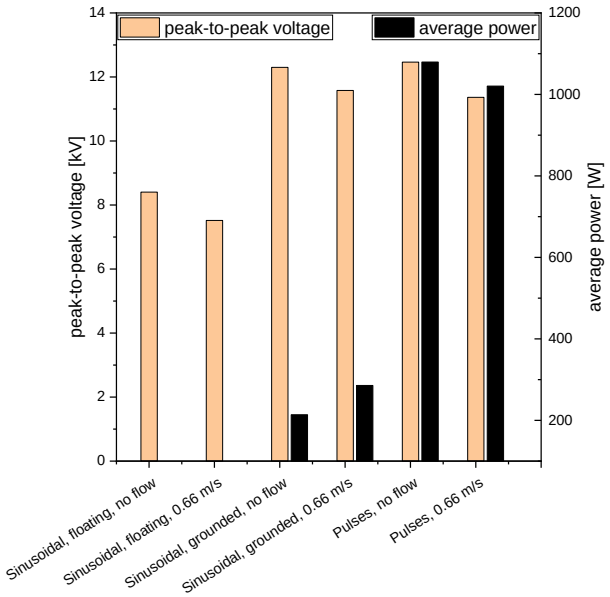


Fig. 3. Measured peak-to-peak voltages and integrated power transfer for both power supplies under different experimental conditions.

The airflow of 0.66 m/s led to a reduction of the peak-to-peak voltages by approx. 5-10 % compared to the values without airflow, regardless of the excitation. The discharge currents and correlated power consumption showed different behaviours: At sinusoidal excitation, the peak currents increased by 25 %, while the average power consumption by the discharge increased by 34 %. At microsecond pulse excitation, however, the peak discharge current remained almost unaffected, while the average

power consumption decreased by 5 %. These effects should most probably originate in transport processes by the gasflow; however, the exact nature of these processes shall be addressed in future investigations.

The reduced electric fields yielded from the OES measurements are presented in Fig. 4. For a direct comparison of the effect of the gas flow, reduced electric fields at 0 m/s (light orange bars) and at 0.66 m/s (black bars) are displayed next to each other at different experimental conditions. Due to the low intensity of light emission from the discharge, however, the stated emission lines just barely exceeded the noise level. Thus, the OES results should be regarded as preliminary findings.

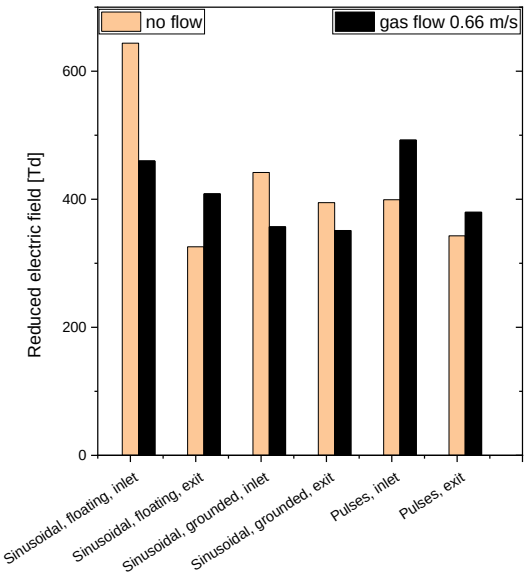


Fig. 4. Reduced electric fields evaluated from OES spectra of the DBD discharges with and without gas flow for sinusoidal and pulsed HV excitation.

The plasma appearance without gas flow showed spatial inhomogeneities, which were most significant for the floating sinusoidal excitation, but were less pronounced for grounded sinusoidal and microsecond pulsed excitation. These appearances are well represented by the values of the reduced electric field compared between inlet and exit of the reactor setup. In all cases of sinusoidal excitation, the inhomogeneity was largely reduced, whereas it increased for the microsecond pulsed excitation. With a typical duration of individual filaments in the order of 10 ns [8], the different effects very likely stem from slower gas transport processes.

The transport processes within the gas flow shall be further discussed by estimating the average travel distances during the high voltage pulse and pause phases of the two different power supplies. For the microsecond pulsed power supply, the average travel distance amounts to approx. 0.4 µm during the HV pulse and approx. 132 µm in-between two pulses. For the sinusoidal excitation, the travel distance amounts to at least 33 µm during the HV phase and less than 100 µm in-between two HV phases. Typical diameters of individual filaments within the discharge are about 0.1 to 1 mm [8], which is approx. the same order of magnitude as in-between two microsecond HV pulses as well as for both phases of the sinusoidal excitation. Therefore, it can be assumed that the transport of gas volume during the breakdown phase of the sinusoidal excitation is responsible for the more homogeneous appearance, whereas the effects of such processes can only influence the conditions prior to the breakdown of the microsecond pulsed discharge.

Photographic images taken by the high speed camera under same illumination and camera settings are shown in Fig. 5. The upper image was taken from a discharge without airflow, whereas for the bottom image, a flowrate of 0.66 m/s of pressurised air from the right border of the image towards the left border of the image was set up. The images illustrate the shift of filaments towards the exit side (left) upon activation of the airflow. The number of filaments further increases near to the reactor's exit when the gas flow is present. Thus, the discharge appears much brighter in case of airflow.

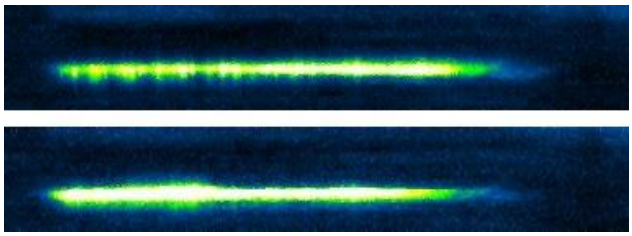

Fig. 5. Optical appearance of the discharge and filament distribution in high-speed camera images without airflow (top image) and at a flowrate of 0.66 m/s (bottom image).

For a two-dimensional discharge setup, the identification of an individual breakdown using a high-speed camera is challenging due to the brightness in front of and behind the camera's focus plane. Setups with reduced complexity overcoming these experimental limitations are either linear edge, or pointes tip electrodes [1,8]. However, gas flow dynamics and their correlation with the plasma are expected to change significantly. Therefore, further detailed insights shall require the support of simulations capturing both, the breakdown dynamics on the nanosecond scale as well as the gas flow dynamics on the microsecond scale.

## 4. Conclusions

The airflow through a planar DBD plasma yielded a reduction of peak voltages by 5 – 10 % at different excitations, while creating a more intense light emission and a high filament density at the reactor exit as compared to the inlet.

Further, for sinusoidal high voltage excitation, when activating the airflow:

- The peak discharge currents increased by 25 %,
- The average power input increased by 34 %, and
- The reduced electric field strengths, on average, significantly decreased, although
- The spatial inhomogeneity of the reduced electric field strength was largely remediated.

Furthermore, for microsecond HV pulses, when activating the airflow:

- The peak discharge currents remained unaffected,
- The average power input decreased by 5 %, and
- The reduced electric field strengths increased notably, while
- The spatial inhomogeneity of the reduced electric field strength significantly increased, thus
- Higher E/N values were observed at the inlet, whereas the discharge at the exit appeared much brighter.

## 5. Acknowledgments

This project has received funding from the European Union's Horizon 2020 research and innovation programme under grant agreement No 745936.
Further, the research received support by the Slovenian Research Agency (project J2-7238 and P2-0082).
The authors gratefully acknowledge the travel funds provided by the German Academic Exchange Service, as well as the provision of equipment by the group of Prof. Maus-Friedrichs at Clausthal University of Technology.

## 6. References

[1] H. Höft, M. M. Becker, M. Kettlitz, Physics of Plasmas, **23**, 033504 (2016).
[2] S. Dahle, W. Maus-Friedrichs, Patent application no. DE 10 2014 226 923.7, submitted on 23.12.2014.
[3] B. Mahdavipour, R. Zaplotnik, M. Panjan, J. Oberrath, S. Dahle. (2019). [Data set]. Zenodo. http://doi.org/10.5281/zenodo.2634048
[4] P. Paris, M. Aints, F. Valk, T. Plank, A. Haljaste, K. V. Kozlov, H.-E. Wagner, Journal of Physics D: Applied Physics, **38**, 3894 (2005)
[5] S. Pancheshnyi Journal of Physics D: Applied Physics, **39**, 1708 (2006)
[6] P. Paris, M. Aints, F. Valk, T. Plank, A. Haljaste, K. V. Kozlov, H.-E. Wagner, Journal of Physics D: Applied Physics, **39**, 2636 (2006)
[7] M. Kuchenbecker, N. Bibinov, A. Kaemlimg, D. Wandke, P. Awakowicz, W. Viöl, Journal of Physics D: Applied Physics, **42**, 045212 (2009).
[8] U. Kogelschatz, IEEE Transactions on Plasma Science, **30**, 1400 (2002).